Evaluating Time-Constant Models in Electrodermal Activity Using Continuous Multi-Frequency Impedance Spectroscopy

Emeric Desmazure, Bertrand Massot, Amalric Montalibet and Claudine Gehin
INSA Lyon, Ecole Centrale de Lyon, CNRS, Universite Claude Bernard Lyon 1, CPE Lyon, INL UMR5270, 69100 Villeurbanne, France

Keywords: Electrodermal Activity, Bioimpedance, Multi-Frequency, Spectroscopy, Cole Parameters, Autonomic Nervous System.

Abstract: A continuous multi-frequency impedance spectroscopy sensor, capable of measuring 16 frequencies, was developed to investigate electrodermal activity. Data was collected from a healthy volunteer over a 30-minute resting period, minimizing interference from the autonomic nervous system. The resulting data were processed with a custom Python algorithm utilizing the ImpedanceFitter library, enabling comparison across models incorporating one, two, and three Cole behaviours. A significant enhancement in accuracy was achieved with the two Cole behaviours over the single Cole behaviour approach, while no additional improvement was observed with a third Cole behaviour. These findings suggest that the two Cole behaviours model provides optimal performance in capturing the complexity of electrodermal activity. Future research will extend this analysis to a larger cohort, exploring how variations in protocol, electrode type, and stimulus may refine the modelling and interpretation of bioimpedance data.

1 INTRODUCTION

Electrodermal activity (EDA) is a physiological function regulated by the autonomic nervous system and is specifically related to signals arising from the activity of sweat glands (Sharkey & Pittman, 1996; Tremblay, 2005). When the autonomic system is activated, it stimulates the sweat glands, which are particularly concentrated in the palmar (hands) and plantar (feet) areas (Matsunaga et al., 1998). This activation leads to increased sweat production within the excretory ducts of the glands (Figure 1), resulting in a greater amount of sweat on the surface of the skin (Goldsmith, 1991). The increase in sweat levels enhances skin conductivity, providing measurable data associated with electrodermal activity

This measurement provides valuable information relevant to psychological state, including conditions such as stress and cognitive load, or psychopathologies such as schizophrenia (Edelberg, 1972). Electrodermal activity is typically measured by placing two electrodes on the palmar or plantar areas, specifically on the distal or middle phalanx or the thenar eminence (Tronstad et al., 2010). A low-intensity, fixed- or zero-frequency alternating or continuous current is passed through the electrodes, with the resulting signal corresponding to skin conductivity. This process is known as exosomatic recoding of electrodermal activity (Fowles et al., 1981) .

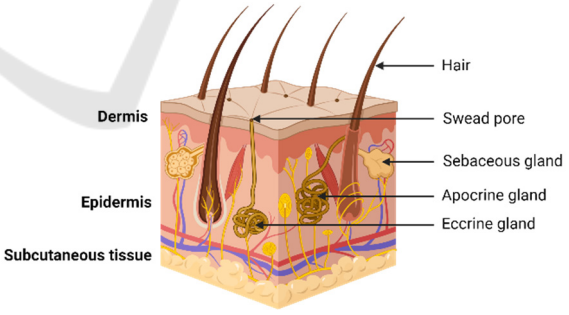

Figure 1: Diagram of skin structure.

A sensor employing impedance spectroscopy in continuous, multi-frequency mode has been developed and validated to comprehensively model skin properties. The device is capable of measuring 8 spectra per second across 16 simultaneous frequencies (f = [12, 28, 32, 36, 44, 68, 84, 108, 136, 196, 256, 342, 400, 484, 576, 724] Hz) continuously. The primary objective is to analyse the data collected by the sensor to enable more accurate model of skin

Desmazure, E., Massot, B., Montalibet, A. and Gehin, C.
Evaluating Time-Constant Models in Electrodermal Activity Using Continuous Multi-Frequency Impedance Spectroscopy.
DOI: 10.5220/0013151400003911

In *Proceedings of the 18th International Joint Conference on Biomedical Engineering Systems and Technologies (BIOSTEC 2025) - Volume 1*, pages 157-162
ISBN: 978-989-758-731-3; ISSN: 2184-4305

properties. This approach is based on the assumption that it is possible to differentiate between the various signals present in the data, such as the electrode-skin interface, tissues and sweat channels. This makes it possible to model electrodermal activity more accurately and faithfully. The signals obtained are in the form of circle, consistent with the classical Cole diagram observed in bioimpedance. Building on this observation and supporting by the literature, modelling incorporating one, two or even three Cole behaviours could refine the analysis (Freeborn et al., 2014). Such a method would facilitate better discrimination between the different components of the signals, thereby optimising the accuracy and fidelity of the modelling.

2 MATERIALS AND METHODS

Data were collected from a volunteer participant in the laboratory. The sensor was positioned on the wrist of the subject's non-dominant hand, while two medium-sized (2.18 x 3.18 mm²) Softrace CONMED electrodes were placed on the distal phalanges of the same hand (Tronstad et al., 2010). The electrodes were connected to the sensor using wires and held in place with adhesive plasters to minimise the electrode-skin interface and ensure optimal contact (Figure 2). No electrode adaptation phase was performed before recording commenced. The subject was invited to lie on a mattress and relax with his eyes closed for approximately 30 minutes. At the end of the protocol, the data were retrieved in the form of CSV files containing temporal information, as well as the real and imaginary parts for the 16 frequencies.

Figure 2 : Sensor and positioning of electrodes on the hand.

2.1 Cole Model

The curves were fitted using the Cole model, which is widely employed in the field of bioimpedance when a Cole diagram is observed. This model is based on an electrical circuit a series resistor (R_s), followed by a parallel combination of a resistor (R_p) and a constant phase element (Z_{CPE}) (Figure 3). It can be used to model various structures, such as tissue, the electrode-skin interface, and sweat ducts.

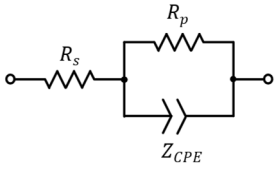

Figure 3: Cole Model.

Cole's diagram provides key parameters, including R_s (resistance at high frequency), R_p (resistance at low frequency), τ (time constant), and α (dispersion factor, which describe how the circle is depressed below the y-axis) (Figure 4).

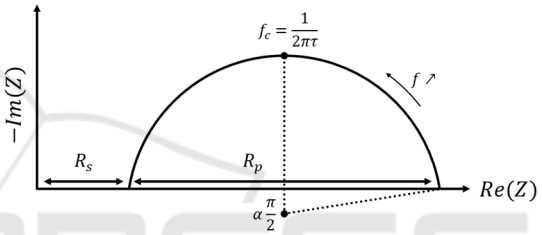

Figure 4: Cole diagram with all Cole parameters.

The aim was to accurately model this system to extract relevant observations. To refine this modelling, the data were analysed by applying one, two or three Cole behaviours to assess their impact and relevance.

The Modelling was carried out using the Python programming language, in conjunction with the ImpedanceFitter library, which allows data to be fitted using models based on one or more of Cole's behaviours. The first spectrum is initialized and fitted using manual values. For all subsequent spectra, the fit is performed automatically, taking the best fit of the previous spectrum as the initial value. This approach is based on the assumption that the variation between successive spectra remains small, allowing very close-fitting results to be obtained. The sensor, as mentioned previously, collects 8 spectra per second, generating several tens of thousands of data points over the 30-minute protocol. An automatic algorithm was developed in conjunction with ImpedanceFitter, enabling the analysis of this vast amount of data in just a few minutes. This algorithm proved to be time saving comparing with manual extraction from a commercial software such as Zview (Scribner).

3 RESULTS

A total of 14,000 spectra were acquired as part of the 30-minute protocol. All the spectra were analysed using one, two or three Cole behaviours. The graphs showing the acquired data and the best fit represent just one arbitrary spectrum from the entire signal. In addition, the error plots show the average of the fitting error over the whole signal for the 16 frequencies.

3.1 One Cole Model

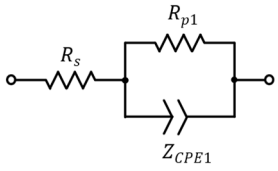

Figure 5: Cole Model – 1 Cole behaviour.

Comparing the curve measured by the sensor with the adjustment made using a single Cole model (Figure 5) for a spectrum, there is a noticeable shift between the real part and the imaginary part at each frequency (Figure 6). This shift results in a relatively high error rate over the entire signal, particularly at high frequencies, ranging from 1% to 30% depending on the frequency (Figure 7). These results suggest the possible presence of additional electrophysiological behaviour in the signals, which justifies the introduction of a second Cole model to improve the fit.

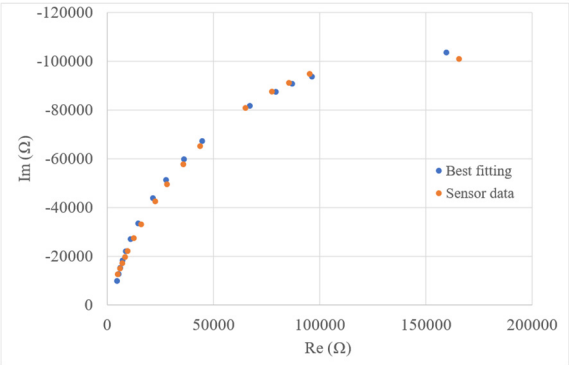

Figure 6: Example of a Nyquist plot of an impedance spectrum acquired (Sensor data) together with the result of a single Cole model fitting.

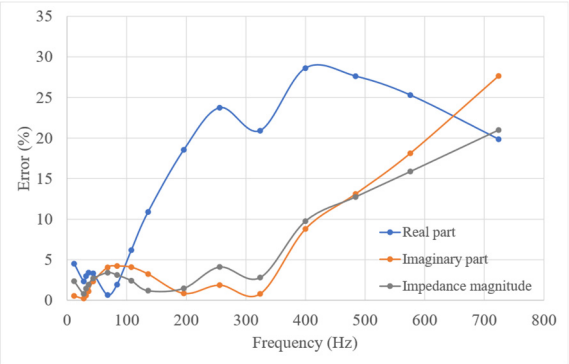

Figure 7: Average error plot the for 1 Cole behaviours over the entire signal.

During the execution of the algorithm, the Cole parameters (R_p, R_s, τ and α) were estimated. It was observed that R_s tended towards 0, a consequence of the limitations of the software, which prevents negative values for R_s from being obtained, as these are biologically impossible (Table 1). Although this constraint is justifiable, it may nonetheless limit the accuracy of the data fit and necessitate improvements to better reflect actual biophysical properties.

Table 1: Cole parameters for one Cole behaviour.

	Cole Parameters
R_s	2.37e^{-24} Ω
R_{p1}	286393 Ω
α_1	0.79
τ_1	10.2ms

3.2 Two Cole Model

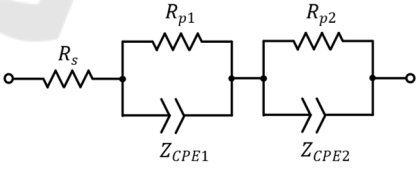

Figure 8: Cole Model – 2 Cole behaviours.

For the same spectrum, the data was then processed using two Cole behaviours (Figure 8). The measured impedance curve, initial values and fit are shown in the graph below (Figure 9). A significant improvement was observed at all frequencies, with a significant reduction in the errors for both the real and imaginary parts. This improvement is further confirmed by the error plot over the whole signal, where the errors approach 0% at low frequencies and 14% at high frequencies, which is halved compared to the fit with a single Cole's behaviour (Figure 10).

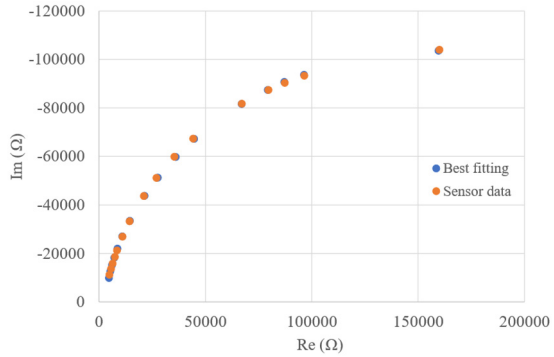

Figure 9: Example of a Nyquist plot of an impedance spectrum acquired (Sensor data) together with the result of a double Cole model fitting.

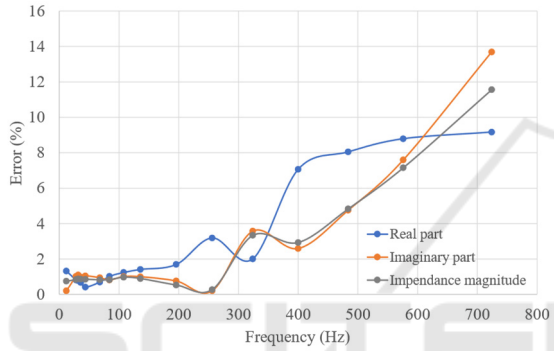

Figure 10: Average error plot the for 2-time constants over the entire signal.

The Cole parameters obtained with two constants showed positive R_s values, consistent with the expected physiological properties, demonstrating the effectiveness of this approach (Table 2).

Table 2: Cole parameters for two Cole behaviours.

	Cole Parameters
R_s	2137 Ω
R_{p1}	117078 Ω
α_1	0.88
τ_1	42.7 ms
R_{p2}	190348 Ω
α_2	0.87
τ_2	23 s

3.3 Three Cole Model

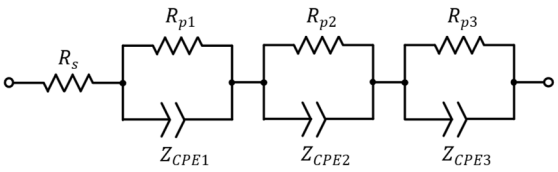

Figure 11: Cole model – 3 Cole behaviours.

Finally, an analysis using three Cole behaviours was performed (Figure 11). However, no significant improvement over the two-constant model was observed (Figure 11). The error rate did not decrease further at low frequencies but increased considerably at high frequencies compared at the 2-time constants (Figure 12). Although the adjustment was always more effective than that obtained with a single time constant (Table 3).

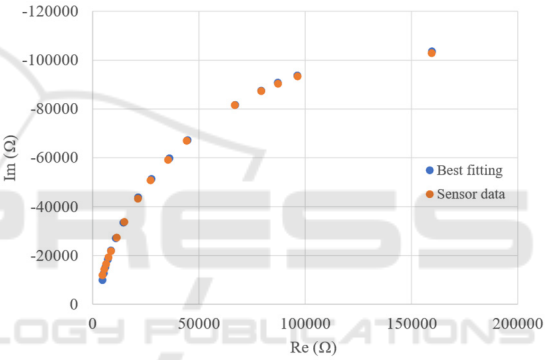

Figure 12: Example of a Nyquist plot of an impedance spectrum acquired (Sensor data) together with the result of a triple Cole model fitting.

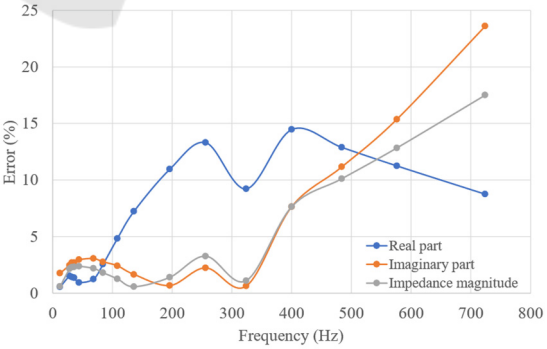

Figure 13: Average error plot the for 3 Cole behaviours over the entire signal.

Table 3: Cole parameters for three Cole behaviours.

	Cole Parameters
R_s	1158 Ω
R_{p1}	134181 Ω
α_1	0.86
τ_1	5 ms
R_{p2}	1349 Ω
α_2	0.79
τ_2	15.5 ms
R_{p3}	183733 Ω
α_3	0.82
τ_3	28.3 ms

4 DISCUSSION

The results obtained confirmed the effectiveness of using two Cole behaviours to accurately model skin conductivity assessed on palms, as performed in the frame of electrodermal activity analysis. When the fit was based on a single Cole behaviour, a significant error rate was observed, particularly at high frequencies, where the differences between the real and imaginary parts were pronounced. This observation suggests that the underlying phenomena, especially at the electrode-skin interface, cannot be fully captured with a single Cole behaviour. These results align with the literature, which indicates that heterogeneous biological systems do not conform to a single Cole model (Lazović et al., 2014). The addition of a second Cole behaviour significantly improved the accuracy of the fit, with a marked reduction in the error rate across all frequencies. In particular, the Rs values, which were close to 0 in the one Cole model due to software constraints, showed a better alignment with physiological realities in the two Cole model. However, a persistent higher error superior at 4% for the high frequency indicates a potential limitation of the device at high frequency. This could be due to interference or hardware artefacts, necessitating further investigation to optimise the device's accuracy at these frequencies. The application of a model with three Cole behaviours showed no significant improvement over the model with two Cole behaviours. This suggests that the use of two Cole behaviour is sufficient to capture the majority of information related to electrodermal activity in this context. However, it remains possible that increasing the precision of the device or exploring more complex experimental contexts could reveal additional electrophysiological phenomena with a three Cole model.

Compared with conventional methods of analysing electrodermal activity, which are limited to the use of a fixed or zero frequency, multi-frequency spectroscopy, combined with dual Cole behaviour modelling, offers a superior capability in analysing skin conductivity. The multi-frequency approach enhances resolution and enables a more accurate analysis of the different electrophysiological components. In the future, it will be investigated if the use of dual Cole behaviour modelling could not only improve the accuracy of skin conductivity modelling in the frame of electrodermal activity analysis, but also provide a better understanding of the underlying physical and physiological mechanisms. By varying the electrodermal stimuli, the duration of the protocol, the subjects studied, or the size and type of electrodes, this approach could provide a more comprehensive view of the system's behaviour. It will be studied if these variations could reveal additional information and refine the interpretation of the electrodermal responses.

5 CONCLUSION

A sensor using continuous multifrequency spectroscopy was designed and validated, enabling more accurate modelling of skin conductivity on palms. Data analysis, based on the assumption of a Cole diagram, was conducted using a Python algorithm built on the ImpedanceFitter library, with fits to one, two and three Cole behaviours. The results demonstrated a significant improvement with two Cole behaviours compared with one, while adding a third behaviours yielded no additional benefit. For future work, the aim will be to collect and analyse new data from different subjects, modifying the protocol to include more stimuli, varying the type or size of electrodes, or adjusting the duration of the protocol, to further refine the modelling of electrodermal activity.

REFERENCES

EDELBERG, R. (1972). Electrical activity of the skin : Its measurement and uses in psychophysiology. *Handbook of psychophysiology*, 367-418.

Fowles, D. C., Christie, M. J., Edelberg, R., Grings, W. W., Lykken, D. T., & Venables, P. H. (1981). Publication Recommendations for Electrodermal Measurements. *Psychophysiology*, *1.*

Freeborn, T. J., Maundy, B., & Elwakil, A. S. (2014). Extracting the parameters of the double-dispersion Cole

bioimpedance model from magnitude response measurements. *Medical & Biological* Engineering *& Computing*, *52*(9), 749-758.

Goldsmith, L. A. (1991). *Physiology, biochemistry, and molecular biology of the skin* (Second edition). Oxford University Press.

Lazović, G., Vosika, Z., Lazarević, M., Simic-Krstić, J., & Koruga, D. (2014). Modeling of Bioimpedance for Human Skin Based on Fractional Distributed- Order Modified Cole Model. *FME Transactions Faculty of Mechanical Engineering, Belgrade*, *42*, 74-81.

Matsunaga, K., Uozumi, T., Tsuji, S., & Murai, Y. (1998). Sympathetic skin responses recorded from non-palmar and non-plantar skin sites : Their role in the evaluation of thermal sweating. *Electroencephalography and Clinical* Neurophysiology/Evoked Potentials Section, 108(5), Article 5.

Sharkey, K. A., & Pittman, Q. J. (1996). The Autonomic Nervous System : Peripheral and Central Integrative Aspects. In R. Greger & U. Windhorst (Éds.), Comprehensive Human Physiology : From Cellular Mechanisms to Integration (p. 335-353). Springer.

Tremblay, J.-M. (2005, février 2). Claude Bernard, Introduction à l'étude de la médecine expérimentale (1865).

Tronstad, C., Johnsen, G., Grimnes, S., & Martinsen, Ø. (2010). A study on electrode gels for skin conductance measurement. Physiological measurement, 31, 1395-1410.